Icarus 374 (2022) 114814

Contents lists available at ScienceDirect

Icarus

journal homepage: www.elsevier.com/locate/icarus

Why was the Kordylewski dust cloud observed more frequently at the L5 Lagrange point than at L4? Asymmetry of the particle capture at the triangular Lagrange points of the Earth-Moon system

Judit Slíz-Balogh [a,b], Bálint Érdi [a], Dániel Horváth [b], Gábor Horváth [b,*]

[a] Department of Astronomy, ELTE Eötvös Loránd University, H-1117 Budapest, Pázmány sétány 1, Hungary
[b] Environmental Optics Laboratory, Department of Biological Physics, ELTE Eötvös Loránd University, H-1117 Budapest, Pázmány sétány 1, Hungary

ARTICLE INFO

Keywords:
Celestial mechanics
Earth
Moon
Triangular Lagrange points L4 and L5
Kordylewski dust cloud

ABSTRACT

In 1961, the Polish astronomer, Kazimierz Kordylewski found dust clouds around the triangular Lagrange points L4 and L5 of the Earth-Moon system. After this discovery, several astronomers observed the Kordylewski dust clouds (KDCs) with photometry or ground-based imaging polarimetry, altogether 21 times. Remarkably, the L5 KDC has been detected three times (16) more than the L4 one (5). This may be due to varying sky and/or astronomical conditions during the KDC observations; for example, the Sun and Moon must be deep enough below the horizon, and the atmosphere must be as aerosol-free as possible. To reveal an additional possible physical reason for the asymmetric frequency of KDC observations, we performed computer simulations. We determined the particle capture at the L4 and L5 points in a 28-day period before the 21 published KDC observations. We found that the L5 point had by maximum 9% larger particle capture than L4, depending on the date of observation. We propose that this bias of the particle capture may be one of the reasons why the KDC has been observed more frequently around the L5 Lagrange point than around L4.

1. Introduction

On 22 February 1906, Maximillian Wolf (cf. Simpson, 1967) discovered 588 Achilles, the first member of the Greek group of asteroids around the L4 Lagrange point of the Sun-Jupiter system. On 17 October of the same year, August Kopff (cf. Simpson, 1967) observed 617 Patroclus, the first asteroid of the Trojan group around Jupiter's L5 Lagrange point. After these antecedents, the Polish astronomer, Kazimierz Kordylewski began to search for similar small solid celestial bodies at the points L4 and L5 of the Earth-Moon system, but his attempt was unsuccessful. From December 1953 to June 1956, Clyde Tombaugh (Tombaugh et al., 1959), the discoverer of Pluto, also searched for small solid bodies around the L4 and L5 points of the Earth-Moon system, again without success. In 1956 the Polish astronomer, Josef Witkowski suggested Kordylewski to look for dust clouds instead of solid bodies. In March 1961 Kordylewski found a dust cloud around the L5 point and another one in September around the L4 point of the Earth-Moon system with naked eyes and photographs (Kordylewski, 1961).

After the discovery of Kordylewski (1961), many professional and amateur astronomers tried to find the Kordylewski dust clouds (KDCs), but without success for a long time. On 4 January 1964 Simpson (1967) and his colleagues (R. G. Miller, G. Gardner) observed the KDC around the L5 point. Thereafter, until 1967 they took about 100 photographs of the KDC, which were too faint for newspaper reproduction, like the pioneering Kordylewski's photos. In 1966 the NASA organized airborne observations of the KDC. During four flights on 1, 2, 10, and 12 March the astronomers on board observed visually and photographically the KDCs. They flew far from city lights at an altitude of 12,000 m and observed both the L4 and L5 KDCs (Simpson, 1967; Vanysek, 1969). Roosen (1966, 1968) did not find the KDC around the L5 point. Wolff et al. (1967) could photograph the L5 KDC from the mentioned NASA aircraft. Using numerical simulations, Röser (1976) investigated the lifetime of dust particles remaining in the vicinity of the Earth-Moon L4 point and the surface brigthness of the L4 KDC. He concluded that the conditions are not favourable for the existence of the KDCs, and therefore he did not believe that these dust clouds exist. Valdes and Freitas Jr. (1983) found no dust clouds around the L4 and L5 points. Roach (1975) and Winiarski (1989) photographed the L5 KDC. Using ground-based imaging polarimetry, Slíz-Balogh et al. (2019) observed the L5 KDC. Table 1 summarizes the details of the published observations and

* Corresponding author.
E-mail address: gh@arago.elte.hu (G. Horváth).

https://doi.org/10.1016/j.icarus.2021.114814
Received 29 July 2021; Received in revised form 13 November 2021; Accepted 17 November 2021
Available online 23 November 2021

Table 1
Dates of published observations and names of observers of the Kordylewski dust cloud around the L4 and L5 Lagrange points of the Earth-Moon system.

L4 observations (5)	L5 observations (16)	observer(s)
	6, 8 March 1961	
	6 April 1961	K. Kordylewski
16, 17, 18 September 1961	3, 4 September 1961	
	4, 6, 7 January 1964	L. W. Simpson, R. G. Miller, G. Gardner
	13 February 1966	L. W. Simpson
	10, 12 March 1966	astronomers of NASA flights (Lockheed plane photography) and L. W. Simpson
1, 2 March 1966	18, 19, 20 February 1976	M. Winiarski
	17, 18 August 2017	J. Slíz-Balogh, A. Barta, G. Horváth

observers of the L4 and L5 KDCs.

It is clear from Table 1, that the L5 KDC has been observed about three times more than the L4 KDC. What can be the reason for this asymmetry? To answer this question, we performed computer simulations, in which we determined the particle capture at the L4 and L5 points in a 28-day period before the published observations of the KDCs listed in Table 1. We found that the L5 point had a maximum of 9% larger dust capture than the L4 point. We propose that this asymmetry can be one of the reasons why the KDC has been observed more frequently around the L5 point than around L4.

Slíz-Balogh et al. (2018) showed that both the radial solar radiation pressure and the Poynting-Robertson (P-R) drag force are negligible relative to the gravitational force for particles with a radius larger than 1 μm, whereas particles with radii of 0.1–0.5 μm can be ejected from the vicinity of the L5 point after a longer period. Consequently, in our present short-term (10 years) simulation we neglected the effects of both forces, which turned out to be unimportant for larger (> 1 μm) particles. Furthermore, based on the simulations of Jorba-Cusco et al. (2021), we assumed that there is no difference in the influence of the solar radiation pressure on L4 and L5.

With their simulations, Salnikova and Stepanov (2020) showed that electric charged particles can form a stable configuration in the first two synodic months in the vicinity of the KDCs. Since in the behaviour of charged particles they did not find any difference between the simulated L4 and L5 dust clouds, we neglected the charge effect. The magnetic effects were also not taken into consideration in our simulations, because – similar to the concentration of charged particles – the concentration of magnetic particles in the KDCs is unknown. Hence, we focused here exclusively on effects of the dominating gravitation. The study of the influence of charge and magnetic effects on the asymmetry between the particle capture of the L4 and L5 KDCs can be an interesting task of future research.

2. Model and methods

Our computations were performed in the heliocentric ecliptic coordinate system Sun-xyz, that is rotated so that the axis x points toward the perihelion of the Earth (Fig. 1). The Sun, Earth and Moon were considered as mass points.

The elliptical motion of the center of mass C of the Earth-Moon system around the Sun was calculated on the basis of the well-known formalism of the two-body problem (Fig. 1). The time-dependent Moon's orbit around the Earth was described by an analytical algorithm developed by Chapront-Touzé and Chapront (1988). The coordinates of the L4 and L5 points were calculated in the orbital plane of the Moon.

The motion of a particle with mass m_p started from the vicinity of the L4 or the L5 point of the Earth-Moon system was described by its equation of motion in the coordinate system Sun-xyz (Fig. 1), taking into account the gravitational influence of the Sun, Earth, and Moon:

$$m_p\ddot{x}_p = -\frac{\partial U}{\partial x_p}, m_p\ddot{y}_p = -\frac{\partial U}{\partial y_p}, m_p\ddot{z}_p = -\frac{\partial U}{\partial z_p} \quad (1)$$

with

$$U = -G\sum_{j=1}^{j=3}\frac{m_p m_j}{r_{pj}}, r_{pj} = \sqrt{(x_p - x_j)^2 + (y_p - y_j)^2 + (z_p - z_j)^2}, j = 1, 2, 3 \quad (2)$$

where x_p, y_p, z_p are the heliocentric rectangular coordinates of the particle (the dot means differentiation with respect to time), $j = 1, 2, 3$ stands for the Sun, Earth, and Moon (main bodies), U is the potential energy of the particle, G is the gravitational constant, m_j ($>> m_p$) is the mass of the main bodies, and r_{pj} is the distance between the particle and the j-th mass. For the Sun $x_i = y_i = z_i = 0$ was assumed, which is an allowable approximation. The exact potential of the particle would be:

$$U^* = -G\sum_{j=1}^{j=3}\frac{m_p m_j}{r_{pj}} - G\sum_{j=2}^{j=3}\frac{m_p m_j}{r_{1j}^3}(\boldsymbol{r_{1j}}\boldsymbol{r_p}), \quad \boldsymbol{r_{1j}} = \boldsymbol{r_1} - \boldsymbol{r_j}, j = 2, 3 \quad (3)$$

if the average distance.

$$\delta = r_{SE}\frac{m_{EM}}{m_{EM} + m_S} = 4.55{\cdot}10^5 \text{ m} \quad (4)$$

of the Sun's center from the center of mass of the Sun-Earth-Moon system were not negligible relative to the Astronomical Unit = r_{SE} = $1.4956{\cdot}10^{11}$ m, where $m_{EM} = 6.0471{\cdot}10^{24}$ kg and $m_S = 1.9891{\cdot}10^{30}$ kg are the mass of the Earth+Moon and the Sun, respectively. The second sum in (3), namely the indirect perturbation of the Earth and Moon, can practically be ignored in our model, because of the negligible distance δ. Our model has the following advanced characteristics: (i) It describes the Moon's very complicated orbit by the Chapront's function (Chapront-Touzé and Chapront, 1988), which takes into consideration not

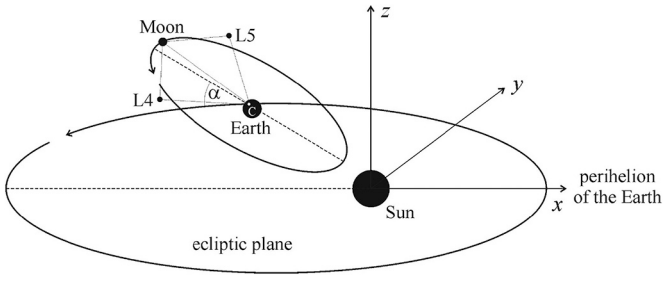

Fig. 1. Not-to-scale schematic drawing of the elliptic orbit (with eccentricity e = 0.0167) of the center of mass C of the Earth-Moon system around the Sun in the plane of the ecliptic, and the elliptic orbit of the Moon and the Lagrange points L4 and L5 of the Earth-Moon system around C in a plane inclined with α = 5.145° to the ecliptic. L4 and L5 are in the vertices of two equilateral triangles formed by the Earth, Moon and L4/L5. L4 leads the Moon and L5 follows it.

only the Sun's gravitational perturbation onto the Moon, but also that of the Venus, Mars and Jupiter. (ii) It considers the fact that the center of mass of the Earth-Moon system moves approximately (with a relative deviation $<10^{-8}$) along an ellipse with excentricity $e = 0.0167$ around the Sun. (iii) It considers the fact that the plane of the Moon's orbit is tilted by 5.145° relative to the ecliptic.

The system of Eq. (1) was converted into a system of first-order differential equations. The latter was numerically integrated by a Runge-Kutta-Fehlberg 7(8) integrator (Fehlberg, 1968) with an adaptive step size determined by the accuracy of 10^{-16}. During these calculations the length and time units were the astronomical unit (AU) and the day (= 86,400 s). Our computer simulations have been run on the ELTE HPC 2019 supercomputer.

The source of the KDC is the uniformly distributed interplanetary dust (Jorgensen et al., 2020). Due to perturbations, the particles trapped at L4 and L5 do not remain there for a long time. Therefore, like in Slíz-Balogh et al. (2018), we considered a particle trapped at L4/L5, if it remained in a spherical shell with origin at the Earth's center for 3650 days (= 10 years) with minimum and maximum radii $r_{\min} = 0.5r_0 \le r \le r_{\max} = 1.5r_0$, where $r_0 = 384{,}400$ km is the average Earth-Moon distance and x_{M0}, y_{M0}, z_{M0}, x_{E0}, y_{E0}, z_{E0} are the initial coordinates of the Moon and the Earth at starting time t_0. After many attempts, we chose this large shell, because particles remaining within this shell for 3650 days (during which many of them have detached from the Lagrange points) form a coherent core for 28 days (≈ 1 lunar month). Considering such a sphere is the established custom in the study of the motion of particles around the Lagrange points. For a given t_0, the equations of motion were solved for 90,000 particles, the starting positions of which were uniformly distributed in a rectangular initial domain centred around L4 and L5 in the orbital plane of the Moon (Fig. 2). The long axis of a given rectangular initial domain (of size 0.0007 AU × 0.00044 AU) was perpendicular to the radius pointing to L4/L5 from the Earth (Fig. 2). The initial velocities of particles were equal to that of L4/L5. The Supplementary Table S1 gives the positions and velocities of the L4 and L5 points for the dates τ_0 of published observations listed in Table 1 (with those of the Earth and Moon).

According to Slíz-Balogh et al. (2018), the particles trapped 28 days earlier than the observation of the KDC (Table 1) contribute only minimally to its structure, because after that time the dust is smoothly distributed. Therefore, we modelled the formation of the KDC as follows:

(i) In the first step, for a given date τ_0 of observation (Table 1), the equation of motion (1) was numerically integrated for 10 years (= 3650 days) for 90,000 particles, the initial positions of which were distributed uniformly in the initial domain (Fig. 2, Supplementary Table S1). After this 10-year simulation, we considered further on only those particles, which remained within the critical spherical shell $r_{\min} = 0.5r_0 \le r \le r_{\max} = 1.5r_0$, where $r_0 = 384{,}400$ km is the average distance of the Moon from the Earth. By this, we selected those particles which have the good fortunate not to escape from the vicinity of the L4/L5 points. They are called as 'trapped particles' henceforth, though they can be anywhere within the mentioned critical shell, sometimes even far from L4/L5. The black dots in Fig. 2A, for example, represent the initial positions of such 'trapped' particles.

(ii) In the second step, for a given date τ_0 of observation (Table 1), we computed only the motion of 'trapped' particles starting from their (black) positions (Fig. 2A) in the initial domain on date $\tau = \tau_0 - i$, that is on the i-th day before τ_0. We followed the motion of these particles up to $\tau = \tau_0$, finally obtaining and depicting their positions at τ_0. These particles constituted a 'particular dust

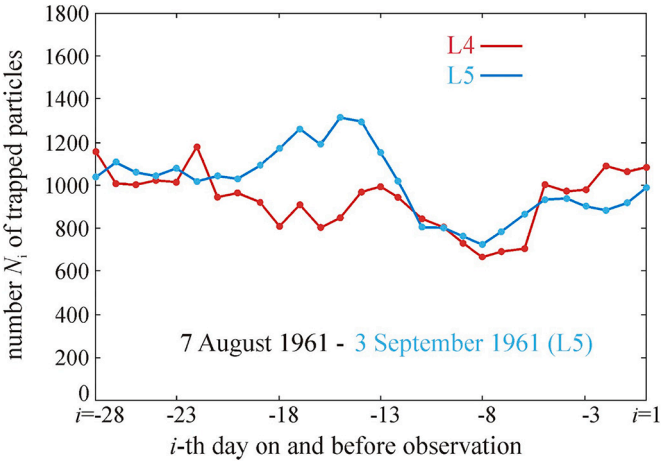

Fig. 3. Numbers $N_{i,L4}$ (red) and $N_{i,L5}$ (blue) of particles ($i = 1, \ldots, 28$) trapped by the Lagrange points L4 and L5 of the Earth-Moon system on the i-th day (= time along the horizontal axis) before 3 September 1961 ($i = 1$) being one of the days of observation of L5 (Table 1). For the sake of better visualization of the temporal change of $N_{i,L4}$ and $N_{i,L5}$, the neighbouring data points are connected with a line as the simplest interpolation. (For interpretation of the references to colour in this figure legend, the reader is referred to the web version of this article.)

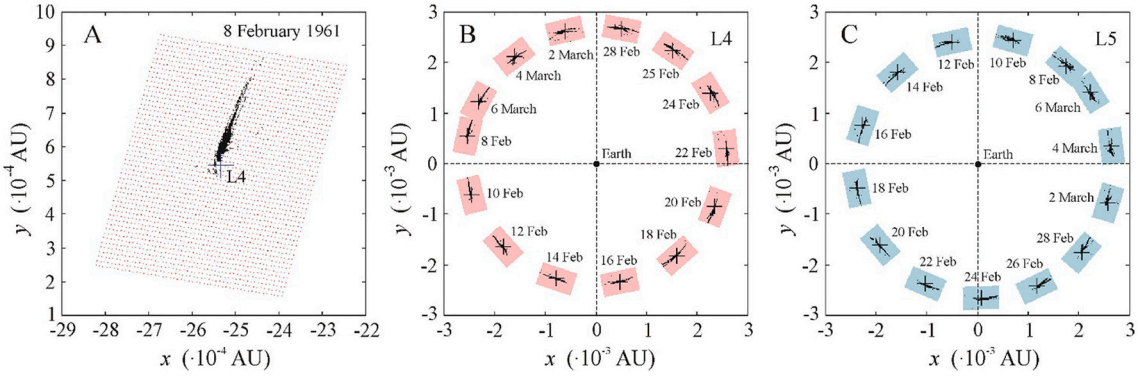

Fig. 2. (A) Initial positions (red dots) of particles around the Lagrange point L4 (black cross) of the Earth-Moon system on 8 February 1961. These positions are in the grid points of a rectangular domain centred around L4. The black dots represent those initial positions of particles which do not escape for 3650 days from the critical spherical shell with minimum and maximum radii $r_{\min} = 0.5r_0 \le r \le r_{\max} = 1.5r_0$, where $r_0 = 384{,}400$ km is the average distance of the Moon from the Earth. (B) Initial domains (red rectangles) of particles around L4 (black cross) belonging to every second day within a 28-day period before 6 March 1961 which was the date of the first observation of the KDC at L5 (Table 1). The Earth is at the origin. (C) Initial domains (blue rectangles) of particles around L5 with the same conditions as in B. All three representations are in a geocentric ecliptic coordinate system. (For interpretation of the references to colour in this figure legend, the reader is referred to the web version of this article.)

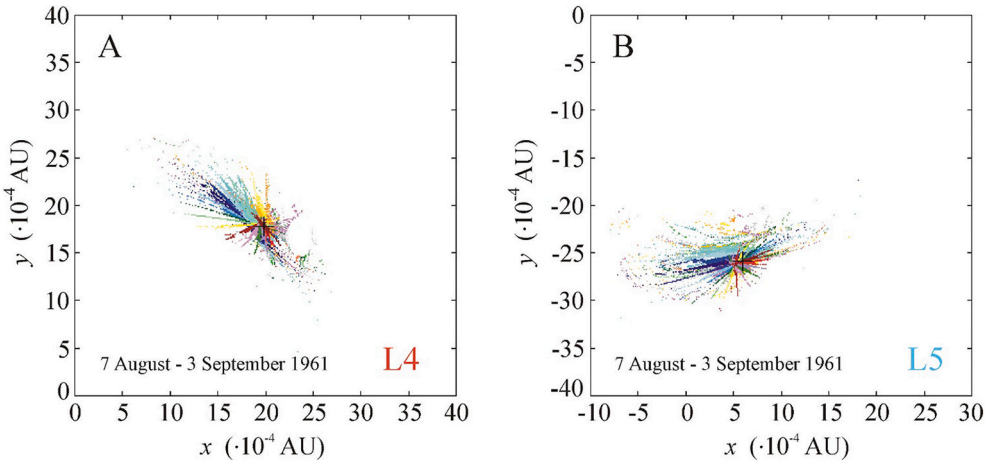

Fig. 4. The summed dust cloud around the Lagrange points L4 (A) and L5 (B) of the Earth-Moon system cumulated within the 27 days before and on 3 September 1961 (being one of the days of observation of L5, Table 1) in a geocentric ecliptic coordinate system *x*-*y* (in Astronomical Unit = AU). The positions of L4 and L5 is represented by a black cross, while the particles trapped on different days are depicted by differently coloured pixels. The three-dimensional interactive versions of these summed dust clouds are available in the Supplementary Stereo Cubes C7 and C8.

cloud' observed on date τ_0, but started on the *i*-th day before τ_0 (Fig. 3). This procedure was performed 28 times for a given date τ_0 (Table 1): for the day of observation ($i = 0$), and for the 27 days ($i = 1, \ldots, 27$, where *i* is the serial number of the day of a particular simulation) before every τ_0. Finally, the obtained 28 different particular dust clouds were summed up and depicted, resulting in the 'summed dust cloud' (Figs. 4, 5). This summed dust cloud was considered as the simulated KDC observed at a given date τ_0 (Table 1).

Of course, on a given date τ_0 there still exist the particles which will escape from the critical shell within 10 years, but remain in this shell for *i* days. These 'non-trapped' particles constitute a homogeneous background ('noise') of the summed up dust cloud (see Fig. 6).

3. Results

Fig. 3 illustrates the numbers $N_{i,L4}$ and $N_{i,L5}$ of particles ($i = 1, \ldots, 28$) trapped by the Lagrange points L4 and L5 of the Earth-Moon system on the *i*-th day before 3 September 1961. Supplementary Fig. S1 shows $N_{i,L4}$ and $N_{i,L5}$ of particles trapped by L4 and L5 on the *i*-th day before the date τ_0 of observation of L4 or L5 for all remaining days of observation (Table 1). Sometimes $N_{i,L4} > N_{i,L5}$ or $N_{i,L4} < N_{i,L5}$, while other times $N_{i,L4} \approx N_{i,L5}$. Many times both curves $N_{i,L4}$ and $N_{i,L5}$ increase or decrease simultaneously with time, but several times they change oppositely (Fig. 3).

Fig. 4 shows the summed dust cloud around L4 and L5 cumulated within the 27 days before and on 3 September 1961 (Table 1). The filamentary structures of both dust clouds are qualitatively similar. Different filaments (coded by different colours) represent different populations of trapped particles. The older the population, the longer is its filament. The same characteristics can be seen in Supplementary Fig. S2 displaying the summed dust clouds around L4 and L5 cumulated within the 27 days before and on the other 20 days of observation (Table 1).

Table 2 contains the total numbers $N_{L4} = \sum_{i=1}^{28} N_{i,\,L4}$ and $N_{L5} = \sum_{i=1}^{28} N_{i,\,L5}$ of particles trapped by L4 and L5 within 27 days before and on τ_0, where $N_{i,L4}$ and $N_{i,L5}$ ($i = 1, \ldots, 28$) are the number of trapped particles on the i-th day before the date of observation of L4 or L5. According to Table 2, N_{L5} is always larger than N_{L4}. Therefore, the quotient $q = (N_{L5} - N_{L4})/N_{L5}$ is always positive ranging between 0.7% and 8.9% (Table 2). This bias of the total number of particles trapped by L4 and L5 demonstrates that the KDC around L5 may be denser than that around L4. However, for the photometric observability of the KDC the density of light-scattering particles is of importance, rather than their number. Therefore, we calculated the numbers $n_{L4}(r)$ and $n_{L5}(r)$ of particles of the summed dust clouds within a sphere with radius *r* centred at L4 and L5 observed on the days listed in Table 1, because the particle density $3n_{L4,L5}(r)/(4\pi r^3)$ is proportional to $n_{L4,L5}$. According to Fig. 5A and Supplementary Fig. S3, sometimes, $n_{L4}(r) \approx n_{L5}(r)$ for $r < 5000$ km (Fig. 5A, Supplementary Figs. S3 E, F, G, I, J, K, L, M, Q, R). More frequently, $n_{L4}(r) < n_{L5}(r)$ for $r > 15{,}000$ km (Figs. 5A,B,C, Supplementary Figs. S3 B, D, E, F, G, H, I, J, K, L, M, N, Q, R). Most often, $n_{L4}(r) < n_{L5}(r)$ for $r < 15{,}000$ km (Figs. 5B,C, Supplementary Figs. S3 A, B, C, E, F, G, H, I, J, K, L, M, N, O, P, Q, R). Since the density of light-scattering particles of the KDC is highest in its core, the latter is the easiest to be observed photometrically. Therefore, considering the visibility of the KDC in L4 and L5, the relation between $n_{L4}(r)$ and $n_{L5}(r)$ is of particular importance for the central region $r < 15{,}000$ km. The fact, that the asymmetry $n_{L4}(r < 15{,}000\text{ km}) < n_{L5}(r < 15{,}000\text{ km})$ dominates, can explain why the KDC has been more frequently observed around L5 than L4 (Table 1).

It should be noted that the uniformly distributed interplanetary dust forms a homogeneous background as shown in Fig. 6 for 6 March 1961. For better visibility of the KDC and due to the assumed homogeneity of the interplanetary dust, this background is neither shown in Figs. 2-5, nor included in Table 2.

On the basis of the above results we propose that the asymmetric particle capture of the L4 and L5 points and the bias of the particle density (Fig. 5, Table 2) can be one of the reasons for the easier observability of the L5 KDC.

4. Discussion

The celestial mechanical problem studied by us in the Sun-Earth-Moon-particle system is a semi-elliptical restricted four-body problem (semi, because the Moon's orbit around the Earth is not an exact ellipse, and the model we used, developed by Chapront-Touzé and Chapront (1988), takes into consideration also the Sun-, Venus-, Mars- and Jupiter-induced perturbations), rather than a circular restricted three-body problem. In this work we showed by numerical simulations that the introduction of (i) an additional mass, the Sun, (ii) the ellipticity of the Earth's and Moon's orbits, and (iii) the tilt angle of the Moon's elliptical orbit (relative to the ecliptic plane) to the circular restricted three-body problem changes the dynamical behaviour of dust particles around the L4 and L5 points. One of the consequences of this is the asymmetry between the numbers of particles and the core density of the L4 and L5 KDCs. We admit that presently we do not understand the exact physical reasons for the development of this asymmetry. Our result obtained by computer simulations could inspire theoreticians to find a physical explanation of this unexpected asymmetry.

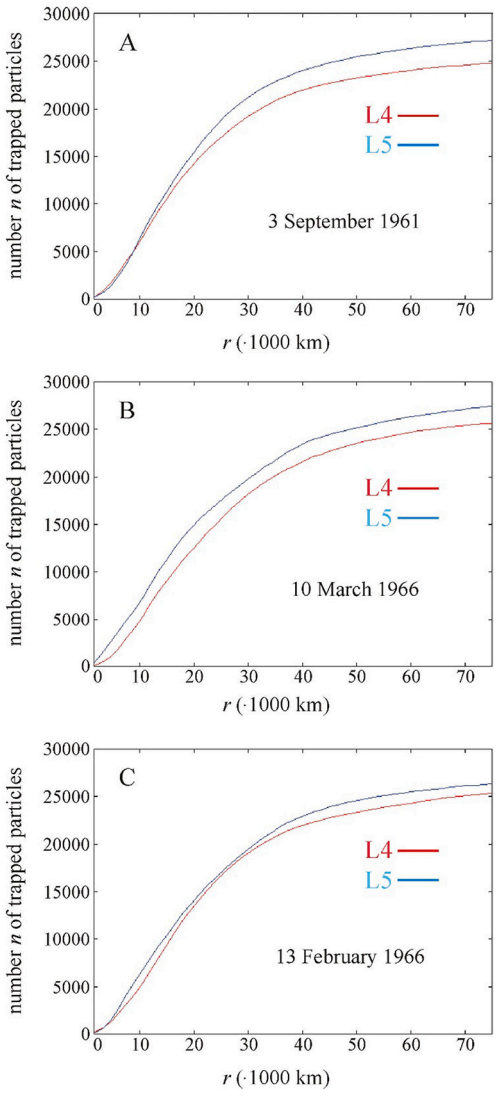

Fig. 5. Numbers n_{L4} (red) and n_{L5} (blue) of particles of the summed dust clouds around L4 (red) and L5 (blue) as a function of the radius r of a sphere centred at L4 and L5 observed on 3 September 1961 (A), 10 March 1966 (B) and 13 February 1966 (C). Although n is depicted here only up to 70,000 km, the capture criterion was that these particles do not escape from the shell with minimum-maximum radii $0.5r_0$–$1.5r_0$ (r_0 = 384,400 km) for 3650 days. (For interpretation of the references to colour in this figure legend, the reader is referred to the web version of this article.)

For an optimal observability of the KDC many environmental conditions have to be satisfied:

(i) The sky must be perfectly cloud- and aerosol-free.
(ii) The Moon must be below the horizon to eliminate the disturbing moonlight scattered in the atmosphere.
(iii) The declination of the Moon should be as high as possible (highest in winter) in order to minimize the light path in the atmosphere and the disturbance of artificial lights.
(iv) The Sun must be more than 18° below the horizon to ensure enough darkness of the sky.
(v) The KDC must not be near the Milky Way, or the antisolar point, or bright celestial objects.
(vi) For photometric observations the phase angle of the KDC (Earth-KDC-Sun) should be near 0°.
(vii) For imaging polarimetric observations the KDC's phase angle should be approximately 90°.

Note that both the L4 and the L5 KDCs cannot be seen on the same night, because the L5 KDC is observable prior to moonrise, while the L4 KDC is detectable only after moonset. Since all these conditions are simultaneously satisfied only very rarely, it is extremely difficult to detect the KDC. According to Table 1, the KDC in the L5 Lagrange point was three times more frequently observed than in L4. On the one hand, one of the reasons of this observational asymmetry could be simply the random selection of appropriate nights of observation. On the other hand, when L5 was in observable position, the above-mentioned environmental conditions might have been more favourable than for L4. However, the hunt for both KDCs happened for decades by several researchers including K. Kordylewski (see Table 1) due to the trendyness of KDCs, therefore in our opinion the threefold asymmetry cannot be explained by the mentioned reasons. Therefore, we examined a possible physical reason: we determined the particle capture of the L4 and L5 points by computer simulations in a 28-day period before the published observations of the KDC (Table 1). Note that most of the previous studies investigated the dust cloud formation around either the L4 (Érdi et al., 2009; Salnikova et al., 2018) or the L5 (Slíz-Balogh et al., 2018) Lagrange point. Therefore, obviously, no asymmetry between their particle capture could have been found.

Montesinos et al. (2020) found also that in protoplanetary disks the total mass of the trapped particles is more significant in L5 than in L4. Lhotka and Celletti (2015) showed the asymmetry of stability of L4 and L5 in the spatial, elliptic, restricted three-body problem applying the effect of Poynting-Robertson drag. Furthermore, let us not forget the well-known asymmetry of Jupiter's Trojan and Greek asteroids (Robutel and Souchay, 2010).

Another reason for the more frequent detection of the L5 KDC may be that the interplanetary dust supply is temporally not uniform. Recently, Jorgensen et al. (2020) analyzed the distribution of interplanetary dust detected by the Juno spacecraft. They found that close to the Earth's orbit – including the triangular Lagrange points and their surroundings – the interplanetary dust is more or less evenly distributed. Thus, in our simulations we assumed a spatiotemporally uniform dust distribution. Remarkably, in spite of the assumed homogeneity, we found a maximum 9% asymmetry between the numbers of particles trapped by the L4 and L5 Lagrange points of the Earth-Moon system.

Fig. 3 and Supplementary Fig. S1 demonstrate well this asymmetry between the numbers of particles captured daily by each triangular Lagrange point. Although this number asymmetry is striking, it says nothing about the local density of the dust cloud, which is the most important considering the observation of KDC. Although L5 trapped maximum 9% more particles than L4 (Table 2), this again does not necessarily mean the easier observability of the L5 KDC compared to the L4 one, because the particle density is of importance as mentioned before.

The estimated radius of the core of the KDC observed around L5 on 17 and 18 August 2017 is about 25,000 km (Slíz-Balogh et al., 2019). Within this radius, the L5-trapped particles are more numerous (in two cases by about 30%, see Supplementary Figs. S3 K,L) than the L4-trapped ones in 17 cases of the 21 simulated summed dust clouds (Fig. 5, Supplementary Figs. S3 A, B, D, E, F, G, H, I, J, K, L, M, Q, R). In the remaining 4 cases (Supplementary Figs. S3 C, N, O, P), the same is true, but only for r = 15,000 km.

Hence, in the case of a uniform and continuous interplanetary dust distribution, L5 captures more particles than L4, and the central core of the former is denser than that of the latter. Consequently, the three-times more frequent observation of the L5 KDC relative to the L4 KDC can also be explained by this purely celestial mechanical finding, beside the random selection of appropriate nights for KDC observation and/or the above-mentioned favorable environmental conditions.

Note that 3 times more particles of the L5 KDC are not necessary at all for its 3 times more frequent observation relative to the L4 KDC: Let the minimum number of core particles necessary to observe a KDC be N_{min}. If the number of core particles N_{L4} of the L4 KDC were smaller than N_{min}

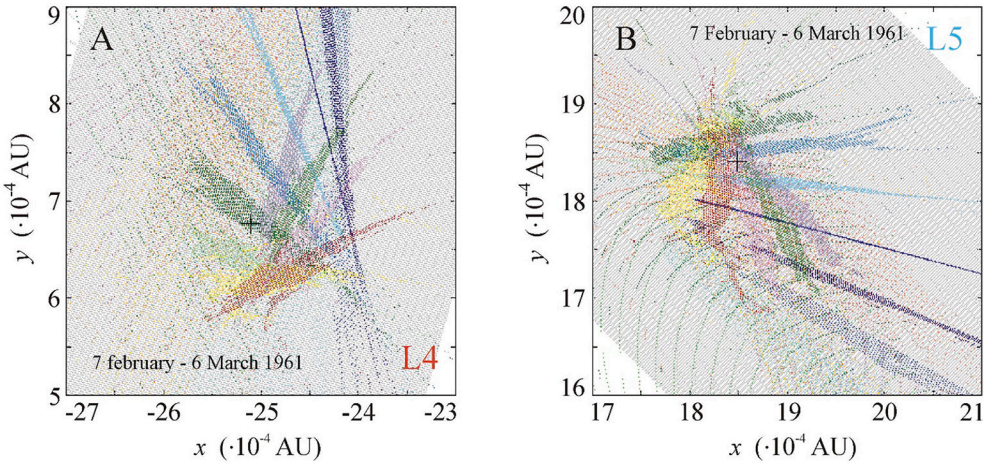

Fig. 6. The core of the summed dust cloud (coloured dots) around the Lagrange points L4 (A) and L5 (B) of the Earth-Moon system cumulated within the 27 days before and on 6 March 1961 together with the uniformly distributed dust-background (grey dots) in a geocentric ecliptic coordinate system *x*-*y* (in Astronomical Unit = AU). The positions of L4 and L5 are represented by a black cross.

Table 2
Column 1 (from left): Date of published observations τ_0 of the Lagrange points L4 and L5 of the Earth-Moon system. *Column 2*: Total number $N_{L4} = \sum_{i=1}^{28} N_{i,\,L4}$ of particles trapped by L4 within 28 days, where $N_{i,L4}$ ($i = 1, \ldots, 28$) is the number of trapped particles on the *i*-th day before the date of observation of L4 or L5. *Column 3*: Total number $N_{L5} = \sum_{i=1}^{28} N_{i,\,L5}$ of particles trapped by L5 within 28 days, where $N_{i,L5}$ ($i = 1, \ldots, 28$) is the number of trapped particles on the *i*-th day before the date of observation of L4 or L5. *Column 4*: Quotient $q = (N_{L5} - N_{L4})/N_{L5}$.

Date τ_0 of observation of L4 or L5	N_{L4}	N_{L5}	q
6 March 1961, L5	27,494	28,753	4.4%
8 March 1961, L5	27,509	28,802	4.5%
6 April 1961, L5	30,318	30,758	1.4%
3 September 1961, L5	26,147	28,236	7.4%
4 September 1961, L5	26,041	28,151	7.5%
16 September 1961, L4	26,567	28,051	5.3%
17 September 1961, L4	26,516	28,084	5.6%
18 September 1961, L4	26,591	28,222	5.8%
4 January 1964, L5	27,298	29,919	8.7%
6 January 1964, L5	27,543	30,023	8.3%
7 January 1964, L5	27,756	30,243	8.2%
13 February 1966, L5	26,071	27,416	4.7%
1 March 1966, L4	26,460	28,207	6.1%
2 March 1966, L4	26,515	28,847	8.0%
10 March 1966, L5	26,382	28,845	8.5%
12 March 1966, L5	26,302	28,891	8.9%
18 February 1976, L5	28,233	28,521	1.0%
19 February 1976, L5	28,275	28,492	0.7%
20 February 1976, L5	28,235	28,544	1.1%
17 August 2017, L5	29,923	30,921	3.2%
18 August 2017, L5	30,140	30,812	2.2%

($> N_{L4}$), but N_{L5} were larger than N_{min} ($< N_{L5}$) by 0.7–8.9%, for example, then L4 could never be observed, while L5 could always be observed under appropriate astrononomical and meteorological conditions. Hence, in principle, a minimal excess number of core particles trapped by the L5 KDC is enough to explain practically any higher observed factor relative to the L4 KDC. Consequently, the obtained 0.7–8.9% excess of the L5 KDC can give rise to the observed factor 3 difference in KDC detections. Since presently the value of threshold N_{min} is unknown, the dependence of the sensitivity of KDC detection on this threshold cannot be quantified. Based on the above argument, a random selection of appropriate nights of observation would be less likely than the found maximum 9% increase of particles at the L5 point over the L4 point.

On the other hand, as an extreme case let us assume that 3-times more or 3-times less particles of a dust cloud would be needed for its 3 times more or 3-times less frequent observation than another dust cloud. Supposing that the starting number N_0 of particles of a dust cloud increases/decreases by increment/decrement $\varepsilon = 0.007$–0.089 (= 0.7–8.9%) in every year/decade/century/millenary, for example, the particle number reaches a 3-times value $3N_0 = (1 + \varepsilon)^n \cdot N_0$ or a 1/3-times value $N_0/3 = (1\text{-}\varepsilon)^n \cdot N_0$ after n years/decades/centurys/millenaries, where $n = \log_{10}(3)/\log_{10}(1 + \varepsilon) \approx 13$–$158$ or $n = \log_{10}(1/3)/\log_{10}(1\text{-}\varepsilon) \approx 12$–$156$. Note that the possibilities of asymmetric capture rates and asymmetric escape rates are equally important.

To find the exact reasons of the asymmetric capture/escape rates of the triangular Lagrange points of the Earth-Moon system specially, and of the Solar Sytem (e.g. the Trojan and Greek asteroids in the Sun-Jupiter system) generally, further computer modellings are necessary. The dynamics of the KDCs of the Earth and Moon should also be studied thoroughly by wide (minimum $15^o \times 15^o$) field-of-view imaging polarimetry in arid regions with ideal (clear-sky, light-pollution-free) astroclimate. Wang et al. (2021) also suggested to continue the ground- and space-based observation of the KDCs.

5. Conclusion

To find a possible celestial mechanical reason for the 3:1 asymmetric frequency of observations of the L5:L4 Kordylewski dust clouds (KDCs) of the Earth-Moon system, we determined the particle capture at the L4 and L5 points in a 28-day period before the 21 published KDC observations. We found that the L5 point had by maximum 9% larger particle capture than L4, depending on the date of observation. This bias of the particle capture may be one of the reasons why the KDC has been observed 3-times more frequently around the L5 Lagrange point than around L4.

Data availability

The data underlying this article are available in the article and in its online supplementary material.

Author contributions

Conceptualization: JSB, GH Data curation: JSB, BÉFormal analysis: JSB, GH Funding acquisition: there was no funding Investigation: JSB, BÉ, GHMethodology: JSB, BÉ, GHProject administration: JSB, GH Resources: JSB, GHSoftware: JSB, BÉ, DH Supervision: BÉ, GH Validation: JSB, BÉ, GHVisualization: JSB, DH, GHWriting - original draft: JSB, BÉ, GH Writing - review & editing: JSB, BÉ, GH

Declaration of Competing Interest

We have no competing interests.

Acknowledgments

We thank the help of Dr. Miklós Slíz (Graphisoft SE, Budapest) in the software development. No funding is declared. We are grateful to Referee 1 (Anthony R. Dobrovolskis), Referee 2 (anonymous) and Referee 3 (Richard Schwarz) for their valuable comments on earlier versions of our manuscript.

Appendix A. Supplementary data

Supplementary data to this article can be found online at https://doi.org/10.1016/j.icarus.2021.114814.

References

Chapront-Touzé, M., Chapront, J., 1988. ELP 2000-85: a semi-analytical lunar ephemeris adequate for historical times. Astron. Astrophys. 190, 342–352.
Érdi, B., Forgács-Dajka, E., Nagy, I., Rajnai, R., 2009. A parametric study of stability and resonances around L_4 in the elliptic restricted three-body problem. Celest. Mech. Dyn. Astron. 104, 145–158.
Fehlberg, E., 1968. Classical fifth-, sixth-, seventh-, and eighth-order Runge-Kutta formulas with stepsize control. NASA Techn. Rep. R-287.
Jorba-Cusco, M., Farres, A., Jorba, A., 2021. On the stabilizing effect of solar radiation pressure in the Earth-Moon system. Adv. Space Res. 67, 2812–2822.
Jorgensen, J.L., Benn, M., Connerney, J.E.P., Denver, T., Jorgensen, P.S., Andersen, A.C., Bolton, S.J., 2020. Distribution of interplanetary dust detected by the Juno spacecraft and its contribution to the zodiacal light. J. Geophys. Res. Planets 126, e2020JE006509.
Kordylewski, K., 1961. Photographische untersuchungen des librationspunktes L5 im system erde-mond. Acta Astronautica 11, 165–169.
Lhotka, C.L., Celletti, A., 2015. The effect of Poynting-Robertson drag on the triangular Lagrangian points. Icarus 250, 249–261.
Montesinos, M., Garrido-Deutelmoser, J., Olofsson, J., Giuppone, C.A., Cuadra, J., Bayo, A., Sucerquia, M., Cuello, N., 2020. Dust trapping around Lagrangian points in protoplanetary disks. Astron. Astrophys. 642, A224.
Roach, J., 1975. Counterglow from the Earth-Moon libration points. Planet. Space Sci. 23, 173–181.
Robutel, P., Souchay, J., 2010. An introduction to the dynamics of Trojan asteroids. Lecture Notes Phys. 790, 195–229.
Roosen, R.G., 1966. A photographic investigation of the L5 point in the Earth-Moon system. Sky Telescope 32, 139.
Roosen, R.G., 1968. A photographic investigation of the gegenschein and the Earth-Moon libration point L_5. Icarus 9, 429–439.
Röser, S., 1976. On the visibility of the libration clouds. In: Elsaesser, H., Fechtig, H. (Eds.), Interplanetary Dust and Zodiacal Light, Proceedings of IAU Colloq. 31, Heidelberg, 10-13 June 1975. Springer, Heidelberg, pp. 124–129.
Salnikova, T., Stepanov, S., 2020. Dust charged particles motion in vicinity of the Lagrange libration points. Adv. Astronaut. Sci. 170, 91–96.
Salnikova, T., Stepanov, S., Shuvalova, A., 2018. Probabilistic model of the Kordylewski dust clouds formation. Acta Astronautica 150, 85–91.
Simpson, J.W., 1967. Dust cloud moons of the earth. Phys. Today 20, 39–46.
Slíz-Balogh, J., Barta, A., Horváth, G., 2018. Celestial mechanics and polarization optics of the Kordylewski dust cloud in the Earth-Moon Lagrange point L5 - I. Three-dimensional celestial mechanical modelling of dust cloud formation. Mon. Not. R. Astron. Soc. 480, 5550–5559.
Slíz-Balogh, J., Barta, A., Horváth, G., 2019. Celestial mechanics and polarization optics of the Kordylewski dust cloud in the Earth-Moon Lagrange point L5 - Part II. Imaging polarimetric observation: new evidence for the existence of Kordylewski dust cloud. Mon. Not. R. Astron. Soc. 482, 762–770.
Tombaugh, C.W., Robinson, J.C., Smith, B.A., Murrell, A.S., 1959. The search for small natural Earth satellites: Final technical report. Phys. Sci. Lab. New Mexico State Univ.
Valdes, F., Freitas Jr., R.A., 1983. A search for objects near the Earth-Moon Lagrangian points. Icarus 53, 453–457.
Vanysek, V., 1969. Detectability of lunar libration clouds at small phase angles. Nature 221, 47–48.
Wang, P., Jiang, X.J., Hou, X.Y., Li, Zhang, H., Jiang, L.X., Wang, J.Q., Zhi, H., Jiao, Z.L., Li, T., Liu, M.H., Wang, J.F., 2021. Ground- and space-based observation of Kordylewski clouds. Space Sci. Technol. 2021, 6597921 https://doi.org/10.34133/2021/6597921.
Winiarski, M., 1989. Photographic observations of the cloud in the neighbourhood of libration point L5 of the Earth-Moon system. Earth Moon Planet. 47, 193–215.
Wolff, C., Dunkelman, L., Hanghney, L.C., 1967. Photograph of the Earth's cloud satellite from an aircraft. Science 157, 427–429.